

Published in final edited form as:

Stroke. 2003 January ; 34(1): 207–213.

Reperfusion Differentially Induces Caspase-3 Activation in Ischemic Core and Penumbra After Stroke in Immature Brain

C. Manabat, BS, B. H. Han, PhD, M. Wendland, PhD, N. Derugin, MA, C. K. Fox, BS, J. Choi, BS, D. M. Holtzman, MD, D. M. Ferriero, MD, and Z. S. Vexler, PhD

From the Departments of Neurology (C.M., C.K.F., D.M.F., Z.S.V.), Pediatrics (D.M.F.), Radiology (M.W.), and Neurosurgery (N.D.), University of California at San Francisco, and Center for the Study of Nervous System Injury, Departments of Neurology and Molecular Biology and Pharmacology, Washington University School of Medicine, St Louis, Mo (B.H.H., J.C., D.M.H.).

Abstract

Background and Purpose—Different strategies for neuroprotection of neonatal stroke may be required because the developing brain responds differently to hypoxia-ischemia than the mature brain. This study was designed to determine the role of caspase-dependent injury in the pathophysiology of pure focal cerebral ischemia in the immature brain.

Methods—Postnatal day 7 rats were subjected to permanent or transient middle cerebral artery (MCA) occlusion. Diffusion-weighted MRI was used during occlusion to noninvasively map the evolving ischemic core. The time course of caspase-3 activation in ischemic brain tissue was determined with the use of an Asp-Glu-Val-Asp-aminomethylcoumarin cleavage assay. The anatomy of caspase-3 activation in the ischemic core and penumbra was mapped immunohistochemically with an anti-activated caspase-3 antibody in coronal sections that matched the imaging planes on diffusion-weighted MRI.

Results—A marked increase in caspase-3 activity occurred within 24 hours of reperfusion after transient MCA occlusion. In contrast, caspase-3 activity remained significantly lower within 24 hours of permanent MCA occlusion. Cells with activated caspase-3 were prominent in the penumbra beginning at 3 hours after reperfusion, while a more delayed but marked caspase-3 activation was observed in the ischemic core by 24 hours after reperfusion.

Conclusions—In the neonate, caspase-3 activation is likely to contribute substantially to cell death not only in the penumbra but also in the core after ischemia with reperfusion. Furthermore, persistent perfusion deficits result in less caspase-3 activation and appear to favor caspase-independent injury.

Keywords

apoptosis; caspases; cerebral ischemia; magnetic resonance imaging, diffusion-weighted; neonate

Stroke during the perinatal period affects central nervous system development and leads to neurological morbidity later in life. Recent data suggest a higher incidence of focal ischemia in neonates compared with the incidence of global cerebral ischemia arising from systemic asphyxia.¹ In the neonate, mechanisms of asphyxia are being extensively studied using a model of hypoxia-ischemia,^{2,3} while mechanisms of arterial ischemic injury without the confounding effect of hypoxia are not fully understood. Different strategies for neuroprotection may be required for neonates because the extent of apoptotic and necrotic cell death depends on both age and the severity of the arterial ischemic insult.⁴ Studies in which a hypoxia-ischemia model

in postnatal day 7 (P7) rodents produced by common carotid artery ligation and global hypoxia was used show that apoptotic and necrotic cell death each account for approximately 50% of brain tissue loss.^{5,6}

Apoptotic cell death is a highly regulated process that in many cases requires activation of caspases, a superfamily of cysteine aspartyl-specific proteases (see Schulz et al⁷ for review). Several of the 14 known mammalian caspases are involved in initiation of the apoptotic cascades, while other caspases are responsible for the execution of apoptosis. Caspase-3, an executioner caspase, is thought to play a central role in apoptosis in a wide variety of cells.⁸ Activated caspase-3 cleaves proteins important in maintaining neuronal process integrity, such as actin and fodrin,^{8,9} and nuclear proteins including DNA-dependent protein kinase, the DNA fragmentation factor/inhibitor of caspase-activated DNase (DFF45/ICAD), and poly (ADP-ribose) synthase (PARP).⁸ The level of inactive caspase-3 in normal forebrain tissue gradually declines during maturation, with high levels present in P7 rat pups and very low levels present in adult rats.¹⁰ Neurons are the predominant cell population that undergo caspase-3-dependent apoptosis, starting several hours after hypoxia-ischemia.^{11,12} Execution of programmed cell death is dependent on new protein and RNA synthesis, mitochondrial function,¹³ and sufficient ATP levels for the activation of the caspase cascade.¹⁴ Recent evidence suggests that although some caspase-3-dependent cell death occurs in the adult brain after ischemia, caspase-dependent death is particularly prominent in the neonatal brain after hypoxic and ischemic insults, including hypoxia-ischemia,^{11,15,16} a combination of permanent middle cerebral artery (MCA) ligation with transient common carotid artery occlusion,¹⁷ or global hypoxiaischemia.⁹ For example, a pan-caspase inhibitor in the latter model decreased brain injury by approximately 50%.⁶

The aim of this study was to determine whether activation of caspase-3 occurs in the ischemic core and perifocal regions after transient focal ischemia in the neonatal brain and whether persistent perfusion deficits after permanent occlusion result in a similar pattern of apoptosis. We used focal ischemia models of transient and permanent MCA occlusion^{18,19} to determine the spatial/temporal activation of caspase-3 in relation to disruption of cerebral homeostasis and the presence of reperfusion. Diffusion-weighted MRI (DW MRI) was used to characterize spatial patterns of injury shortly after occlusion and to identify the ischemic core and penumbra. Our data show that neuronal caspase-3 activation occurs robustly in both the ischemic core and penumbra after transient focal ischemia. Furthermore, the temporal patterns and degree of caspase-3 activation depend on disturbances in cerebral blood flow coupled with the presence of reperfusion, which markedly increase caspase-3 activation in lesioned regions.

Materials and Methods

Animal Model

All animal research was approved by the University of California at San Francisco Committee on Animal Research and was performed in accordance with the *Guide for the Care and Use of Laboratory Animals*, US Department of Health and Human Services, Publication No. 85-23, 1985. Sprague-Dawley rats with a 6-day-old litter (10 pups per litter) were obtained from Simonson Labs (Gilroy, Calif). The mother and pups were given food and water ad libitum and housed in a temperature/light-controlled animal care facility. P7 rat pups (weight, 14.7±1.5 g) were subjected to MCA occlusion.^{18,19} Briefly, surgical procedures were performed in spontaneously breathing rats under temperature-controlled conditions with the use of 1% isoflurane in a mixture of 30% O₂ and 70% N₂O. The right common carotid artery was exposed, and the right external carotid artery was ligated. A coated monofilament polypropylene suture (7-0) was advanced through an incision in the external carotid artery to occlude the MCA and was secured. In sham-operated rat pups, the suture was inserted but not advanced. Rat pups were monitored carefully to make sure that they fed and remained hydrated. The suture was

either left in to produce permanent MCA occlusion or removed 3 hours after MCA occlusion to reestablish flow.

MRI Examination and Measurements of Regions of Interest

Echo-planar DW MRI was conducted to document injury and to provide a guide for selecting core and penumbral zones. All animals were imaged between 2 and 2.75 hours after MCA occlusion. Images with heavy diffusion-sensitizing gradient in 4 coronal sections that cover the entire MCA vascular territory were acquired in a field of view of 30 mm according to the standard Stejskal-Tanner method for spin echo, as previously described.¹⁹ Pups with unaltered signal on a single image with heavy diffusion-sensitizing gradient in the entire hemisphere ipsilateral to MCA occlusion were excluded from the study. If hyperintensity was observed in the MCA territory, apparent diffusion coefficient (ADC) maps were constructed by acquiring a set of 9 images with increasing diffusion gradient amplitude.

The ADC-based measurements of the size of the ischemic core and penumbra were performed as follows: the ranges of the lowest ADC values and ADC values in the matching contralateral anatomic regions were derived from the ADC maps such that the region with ADC values lower than the mean of the lowest ADC values plus 1 SD was referred to as the core. The region with ADC values higher than the mean of the ADC values plus 1 SD in the core but lower than the mean of normal ADC values minus 2 SDs in that region was referred to as the ischemic penumbra. The size of the core was expressed as a percentage of the ipsilateral hemisphere area (NIH Image Software) and compared with the size of region containing the CM1-immunoreactive cells. DW MRI was used to guide dissection of affected and matching control regions for Asp-Glu-Val-Asp (DEVD) cleavage assay and Western blot.

DEVD Cleavage Assay

Asp-Glu-Val-Asp-aminomethylcoumarin (DEVD-AMC) cleavage assay was performed as previously described.¹¹ Rats were killed 3, 8, 18, or 24 hours after reperfusion (n=3 to 5 per group) or 7, 11, or 27 hours after permanent MCA occlusion (n=4 to 5 per group). Brains were quickly removed, and tissues from the ischemic region and the matching contralateral anatomic regions were dissected on ice, flash-frozen, and used in the DEVD assay and Western blots. Half of the tissue samples were homogenized in buffer containing 10 mmol/L HEPES (pH 7.4), 42 mmol/L KCl, 5 mmol/L MgCl₂, 1 mmol/L dithiothreitol, 1% Triton X-100, 0.5% CHAPS, 1 mmol/L phenylmethylsulfonyl fluoride, and 1 µg/mL leupeptin and centrifuged at 12 000g for 10 minutes at 4°C. A 10-µL aliquot of the lysate was incubated in a 96-well plate with 90 µL of buffer containing 10 mmol/L HEPES (pH 7.4), 42 mmol/L KCl, 5 mmol/L MgCl₂, 1 mmol/L dithiothreitol, 1% Triton X-100, 0.5% CHAPS, and 10% sucrose and containing 30 µmol/L Ac-DEVD. The fluorescence was measured every 5 minutes for 30 minutes at room temperature at the excitation wavelength of 360 nm, and emission was measured at 460 nm with the use of a multiplate fluorescence reader (Biotek Instruments). Protein concentration was measured with a Pierce kit. Ac-AMC was used to obtain a standard curve. Enzyme activity was calculated as picomoles per minute per milligram protein.

Western Blot Analysis

Fresh-frozen tissue was homogenized in ice-cold buffer containing 20 mmol/L Tris (pH 7.4), 150 mmol/L NaCl, 1 mmol/L EDTA, 1 mmol/L EGTA, 1% Triton X-100, 2.5 mmol/L sodium pyrophosphate, 1 mmol/L sodium orthovanadate, 1 µg leupeptin, and 1 mmol/L Pefablock, and homogenates were centrifuged at 12 000g for 10 minutes. Protein concentration was normalized in supernatant from each brain sample (Pierce kit). Samples were boiled for 5 minutes, subjected to SDS-PAGE (40 µg of protein per lane), and transferred to nitrocellulose (Amersham). Blots were rinsed with 1×Tris-buffered saline (TBS) and 0.1% Tween (TTBS), blocked with 5% milk/TTBS for 1 hour, and probed with primary antibody against cleaved

caspase-3 (1:1000, overnight, 4°C; Cell Signaling, Inc). Blots were stripped and reprobed with antibody against total caspase-3 (1:8000, overnight, 4°C; BD Biosciences, Inc). Appropriate secondary horseradish peroxidase–conjugated antibodies (1:2000, 1 hour, room temperature, Cell Signaling, Inc) were used, and signal was visualized with ECL (Amersham).

Immunohistochemistry

Rats were killed 0, 1, 4, 8, or 24 hours after reperfusion (n=3 to 4 per group) by perfusion-fixation with ice-cold 4% paraformaldehyde in 0.1 mol/L PBS (pH 7.4). Brains were removed, post-fixed for 24 hours, and cryoprotected with 30% sucrose/PBS (72 hours, 4°C); then 2 to 3 coronal sections through MCA territory were cut, flash-frozen with the use of isobutanol/dry ice mixture, and stored at –70°C. Histological sections that matched DW MRI sections were identified, and serial 50- μ m-thick coronal sections were cut with a freezing sliding microtome. Cresyl violet staining and immunohistochemistry were performed on adjacent sections. Peroxidase immunohistochemical staining was performed on free-floating sections with the use of the rabbit polyclonal anti-active caspase-3 CM1 antibody (1:20 000, gift of Idun, Inc) with the ABC Elite kit and visualized with diaminobenzidine as previously described.¹¹

Densitometric Analysis and Quantification of CM1-Immunoreactive Cells

The number of CM1-immunoreactive cells was measured in the developing ischemic core and in penumbra in 2 coronal sections per brain at the levels of plates 11 to 15 from a rat atlas²⁰ with a Zeiss inverted microscope ($\times 5$ objective) and OpenLab Software (Improvision, Inc). Data were averaged per brain. Since precise colocalization of regions with moderately decreased ADC and on the corresponding histochemical slide was difficult, we counted CM1-immunoreactive cells only in the field of view where we were able to reliably identify anatomic features present within the respective sections. Cells were counted in 3 random fields of view of identical size in the core, penumbra, or matching contralateral region per section. Since some cells were clearly identifiable morphologically as neurons, while other cells were round and shrunken, these cell populations were counted separately. The size of the regions that contained CM1-immunoreactive cells after MCA occlusion was determined at $\times 1$ and expressed as percentage of ipsilateral hemisphere.

Immunofluorescence Labeling

Tissue sections were blocked with 3% goat serum in TBS and incubated overnight with mouse anti-neuronal nuclei (1:100) antibody (NeuN, Chemicon, Inc) and CM1 (1:5000). After they were washed, secondary antibodies conjugated to the fluorescent markers Alexa-488 and Alexa-568 (Molecular Probes) were applied to sections for 1 hour. Sections were then washed, mounted on slides, coverslipped with Vectashield mounting media (Vector, Inc), and examined with a Zeiss LSM 5 Pascal confocal microscope.

Statistical Analysis

Statistical analysis was accomplished with the use of factorial 2-way ANOVA and post hoc significance testing with the Fisher test (Statview V, Abacus Software). Data, expressed as mean \pm SD, were considered significant when $P < 0.05$ was achieved.

Results

MRI-Based Delineation of Early Postischemic Injury in P7 Rats

A spatial pattern of injury was determined in each pup 2 to 3 hours after MCA occlusion with the use of DW MRI and derived ADC maps (Figure 1A). The severity of initial injury was graded in the core and in ischemic penumbra on the basis of the difference in ADC values in these regions. Boundaries around the ischemic core and penumbra for representative brain

sections are shown in Figure 1B. ADC values were 0.89 ± 0.09 cm²/s (Figure 1C) in the contralateral cortex and 0.36 ± 0.05 cm²/s in the core. The core occupied $39.5 \pm 6.5\%$ of the ipsilateral hemisphere in a coronal plane containing the caudate. In penumbra, ADC values that met methodological criteria were in the range of 0.54 ± 0.12 cm²/s. ADC maps and the corresponding spatial distribution of activated caspase-3 (CM1-immunoreactive cells) in the same brains are shown in Figure 3.

Activation of Caspase-3 After Transient and Permanent MCA Occlusion in P7 Rats

DEVD-AMC cleavage activity was significantly higher in the ischemic tissue 8 hours after reperfusion than in the matching contralateral anatomic region of the same brain (Figure 2A; $P < 0.005$). Caspase activity continued to increase over time and was approximately 36 times higher in ischemic tissue compared with that in the contralateral hemisphere 24 hours after reperfusion ($P < 0.001$). In contrast to transient MCA occlusion, where caspase-3-like activity progressively increased over the 24-hour postreperfusion period, caspase-3-like activity remained significantly lower after similar periods of permanent occlusion ($P < 0.004$). No increase in DEVD-AMC cleavage activity was observed in the injured tissue at 7 hours after permanent MCA occlusion (Figure 2A). A peak of activity was seen at 11 hours of permanent occlusion and was approximately 5 times lower at 27 hours after permanent MCA occlusion than activity at 24 hours of reperfusion (Figure 2A). Caspase-3-like activity remained at basal levels in the contralateral hemisphere of pups subjected to either transient or permanent occlusion and was not significantly different at various time points. Caspase-3-like activity was also at basal levels in sham-operated pups (not shown). Cleavage of caspase-3 in ischemic tissue was confirmed by Western blot analysis. Pro-caspase-3 expression (an ≈ 32 -kDa band) was observed in both ischemic tissue from the ipsilateral hemisphere and normal tissue from the contralateral hemisphere (top panel, Figure 2B), while caspase-3 cleavage occurred in ischemic but not in normal tissue (bottom panel, Figure 2B). Consistent with the results of the DEVD assay, cleavage was most profound at 18 to 24 hours of reperfusion and at this point was associated with almost complete loss of pro-caspase-3. Relative to transient MCA occlusion, both cleavage of caspase-3 (Figure 2B) and its activation (Figure 2A) were lower after permanent occlusion, and a lesser caspase-3 activation was associated with a more severe injury (Figure 2C). While both transient and permanent MCA occlusion produced substantial injury (Figure 2C), permanent occlusion caused a consistently more severe injury. It was not feasible to measure the size of the infarct, however, since tissue after 24 to 27 hours of permanent occlusion was very fragile.

Time Course of Caspase-3 Activation (CM1 Immunoreactivity) in Ischemic Core and Penumbra

To examine caspase-3 activation in individual cells, selected coronal sections within imaging planes were immunostained with the CM1 antibody, an antibody specific for the activated forms of caspase-3 and -7.²¹ There is abundant caspase-3 in the P7 rat brain and, according to previously published¹¹ and our unpublished data (D.M. Holtzman, 2002), little, if any, caspase-7; therefore, CM1-immunoreactive cells represent predominantly activated caspase-3. Figure 3 shows ADC maps and the corresponding expression of the cleaved caspase-3 in the same animals at various time points after reperfusion. Since CM1-immunoreactive cells formed a boundary around the injured region (Figure 3 and Figure 4), we used the positive cells as a boundary to measure the size of the injured region at 3, 8, and 24 hours after reperfusion. The sizes were $46 \pm 17\%$, $41.9 \pm 12.6\%$, and $35.1 \pm 5.2\%$ of the hemisphere ipsilateral to the occlusion, respectively, and were not significantly different from each other. Because precise anatomic coregistration of MR data and histology is difficult, paired comparisons of sizes of the regions with altered ADC and regions with CM1-immunoreactive cells in sections that matched image sections were performed for each brain. The size of the core as identified by the ADC drop

correlated with the size of regions outlined by the presence of CM1-immunoreactive cells ($P < 0.001$, paired t test).

In the injured hemisphere, a maximum of 1 to 2 CM1-immunoreactive cells per hemisphere was observed 0 and 1 hour after reperfusion (data not shown). CM1-immunoreactive cells became apparent there 3 hours after reperfusion (Figure 3B and Figure 4). Spatial ADC and CM1 maps (Figure 3A and 3B) showed that caspase-3 cleavage first occurred in individual neurons, as well as clusters of neurons, within the penumbra, while CM1-immunoreactive cells were more dispersed in the core than in penumbra (Figure 3B and 3C). By 8 hours of reperfusion, the number of CM1-immunoreactive cells increased in the core (Figure 3D versus Figure 3E and 3F). The CM1-immunoreactive cells increased in the core, and the number remained significantly higher in penumbra (Figure 4; $P < 0.05$). At 24 hours after reperfusion, the number of CM1-immunoreactive cells increased significantly in the core and to a lesser extent in penumbra (Figure 3I, 3J, and Figure 4). Activated caspase-3 was seen in both morphologically intact neurons (Figure 3G and 3J) and neurons undergoing various stages of apoptosis (Figure 3F and 3J). Both neuronal bodies and their processes were intensely stained (Figure 3G). Double-label immunofluorescence with the neuronal marker NeuN and CM1 antibody confirmed that, in injured tissue, NeuN-immunoreactive cells were the predominant population of cells undergoing caspase-3 cleavage (Figure 3J). CM1-immunoreactive cells were only rarely seen in the opposite hemisphere at any time point (Figure 4).

Since both morphologically intact cells as well as cells undergoing advanced stages of cell death were CM1-immunoreactive (Figure 3 and Figure 4), cells that were clearly identifiable as neurons on the basis of morphological criteria (shape and the presence of processes) as well as immunoreactive cells that were small, round, and lacked other neuronal features were counted. When evaluated in this way, approximately 75% of CM1-immunoreactive cells in the core and 69% cells in the penumbra retained clear neuronal features 4 hours after reperfusion. The number of CM1-immunoreactive cells identifiable as neurons declined over time and constituted approximately 11% of CM1-immunoreactive cells in the core and 12% in the penumbra 24 hours after reperfusion. At this point, the majority of cells with activated caspase-3 immunoreactivity were shrunken, suggesting that they were undergoing the terminal phase of apoptotic execution and that a relatively small number of neurons enter caspase-dependent apoptosis by 24 hours of reperfusion.

Discussion

This study demonstrates that caspase-3 activation is prominent in the injured neonatal brain after focal transient arterial ischemia and that while early postreperfusion activation of caspase-3 is more rapid in the penumbra, a more delayed but marked caspase-3 activation occurs in the core by 24 hours of reperfusion. In addition, caspase-3 activity is significantly lower after permanent ischemia.

DW MRI was used to delineate injury 2 to 3 hours after MCA occlusion because we have previously shown that the ADC drop is predictive of infarction after transient MCA occlusion in P7.¹⁹ Absolute ADC values in normal neonatal brain are higher^{22,23} and relative reduction of ADC in postischemic versus normal brain tissue is more profound in neonatal^{19,24} than in adult brain.^{25–28} Using an MRI-derived definition of core and penumbra, we determined that caspase-3 cleavage occurs in both regions but with different dynamics. Since coregistration of individual immunohistochemical sections that correspond to an MRI section is difficult because of changes in brain shape during tissue processing, anatomic landmarks were used to identify the corresponding sections. Using paired t tests, we showed a correlation between size of the core on DW MRI and regions with CM1-immunoreactive cells. Double staining with the neuronal marker NeuN and the CM1 antibody showed that, as in the case of the hypoxia-

ischemia model,¹¹ caspase-3 cleavage occurs predominantly in neurons and that cleavage begins when neurons appear morphologically normal. Caspase-3 activation measured independently by DEVD assay and caspase-3 cleavage measured by Western blot analysis confirmed that activation was restricted to the ischemic/reperfused tissue.

In the areas of moderate ADC reduction (penumbra), the number of CM1-immunoreactive cells was higher than in the core at 3 to 8 hours after reperfusion and continued to increase over time, reaching similar numbers in both areas at 24 hours of reperfusion. It would be important to know the evolution of the cerebral blood flow disturbance in relation to the ADC decrease in the penumbra, but difficulty in obtaining the temporospatial profile of cerebral blood flow in neonatal rats precluded these measurements.

The presence or absence of recirculation in models of transient and permanent MCA occlusion in P7 rats allows direct comparison of the role of reperfusion in triggering mechanisms that contribute to neonatal brain damage. Caspase-3-like activity increased gradually within 24 hours in the core after transient MCA occlusion but was overall lower in the nonperfused core after permanent occlusion, suggesting that caspase-3 activation depends on reperfusion. Accumulation of macrophages or astrocytes is unlikely to account for differences in caspase activity,¹⁹ while reperfusion may play a permissive role for apoptosis to occur by restoring ATP and subsequent protein synthesis. Activation of caspase-3 occurs via mitochondria-dependent and -independent pathways, caspase-9 – dependent pathways. Since postischemic activation of caspase-3 ultimately depends on the severity of the initial injury, a relative activation of caspase-8 and caspase-9 cascades after hypoxia-ischemia in the immature brain may be important.^{15,29,30} Furthermore, apoptosis may be aborted by mechanisms that are poorly understood.³¹ Recent evidence suggests that molecular markers besides caspase-3 may differentiate necrotic from apoptotic death. For example, in the P7 mouse hypoxia-ischemia model, 50% of cell death is caspase-3 independent.⁵ Neurons dying via non-caspase-3-dependent death accumulate the glycoprotein clusterin, lack caspase-3 activation, and do not undergo apoptosis, while cells with cleaved caspase-3 do not accumulate clusterin.

The relationship between age and postischemic caspase-3 activation is not completely understood. Importantly, caspase-3 activity after transient focal cerebral ischemia in immature rats is orders of magnitude higher than that which occurs after hypoxia-ischemia in older rats.^{4,32,33} Similar to this report, a large amount of caspase-3 activation was also reported 12 to 48 hours after hypoxia-ischemia in P7 rats.^{5,11} Use of other assays such as terminal deoxynucleotidyl transferase-mediated dUTP-biotin nick end-labeling (TUNEL) and electron microscopy supports morphological evidence of apoptotic-like changes within 24 hours of hypoxia-ischemia in P7 rodents,^{11,15,16,34} as well as after a combined MCA ligation with transient common carotid artery occlusion.^{17,35} A possible explanation for an age-related difference in caspase-3 activation is the presence of higher levels of pro-caspase-3 at P7.^{10,36} Other possible mechanisms include a different postreperfusion microcirculatory profile in young versus old animals or a differential ability to maintain energy homeostasis. In contrast to transient ischemia in mature brain, where a secondary postreperfusion decline in blood flow occurs within hours after reperfusion,³⁷ brain regions with restored perfusion in P7 rats¹⁹ remain well perfused for at least 24 hours.³⁸ This provides an environment in which ATP can be maintained and intracellular homeostasis can be restored.

Knowledge of temporospatial dynamics of caspase-3-dependent apoptosis leads to potentially important implications for developing therapeutic strategies specifically for neonatal stroke. Further information on the ability to attenuate injury by inhibiting signaling cascades upstream of caspase-3 activation should reveal the functional role of apoptosis inhibition for treatment of this devastating event.

Acknowledgments

This work was supported by American Heart Association, Western Affiliate grants 9960004Y and 0160043Y (Dr Vexler) and by National Institutes of Health grant P50 35902 (Drs Ferriero and Holtzman). The authors thank Dr George Gregory for useful discussions and Ann Sheldon for editorial help.

References

1. Lynch JK, Hirtz DG, DeVeber G, Nelson KB. Report of the National Institute of Neurological Disorders and Stroke workshop on perinatal and childhood stroke. *Pediatrics* 2002;109:116–123. [PubMed: 11773550]
2. Levine S. Anoxic-ischemic encephalopathy in rats. *Am J Pathol* 1960;36:1–17. [PubMed: 14416289]
3. Rice JED, Vannucci RC, Brierley JB. The influence of immaturity on hypoxic-ischemic brain damage in the rat. *Ann Neurol* 1981;9:131–141. [PubMed: 7235629]
4. Marks N, Berg MJ. Recent advances on neuronal caspases in development and neurodegeneration. *Neurochem Int* 1999;35:195–220. [PubMed: 10458652]
5. Han BH, DeMattos RB, Dugan LL, Kim-Han JS, Brendza RP, Fryer JD, Kierson M, Cirrito J, Quick K, Harmony JA, Aronow BJ, Holtzman DM. Clusterin contributes to caspase-3-independent brain injury following neonatal hypoxia-ischemia. *Nat Med* 2001;7:338–343. [PubMed: 11231633]
6. Cheng Y, Deshmukh M, D'Costa A, Demaro JA, Gidday JM, Shah A, Sun Y, Jacquin MF, Johnson EM, Holtzman DM. Caspase inhibitor affords neuroprotection with delayed administration in a rat model of neonatal hypoxic-ischemic brain injury. *J Clin Invest* 1998;101:1992–1999. [PubMed: 9576764]
7. Schulz JB, Weller M, Moskowitz MA. Caspases as treatment targets in stroke and neurodegenerative diseases. *Ann Neurol* 1999;45:421–429. [PubMed: 10211465]
8. Nicholson DW, Thornberry NA. Caspases: killer proteases. *Trends Biochem Sci* 1997;22:299–306. [PubMed: 9270303]
9. Pulera MR, Adams LM, Liu H, Santos DG, Nishimura RN, Yang F, Cole GM, Wasterlain CG. Apoptosis in a neonatal rat model of cerebral hypoxia-ischemia. *Stroke* 1998;29:2622–2630. [PubMed: 9836776]
10. Hu BR, Liu CL, Ouyang Y, Blomgren K, Siesjo BK. Involvement of caspase-3 in cell death after hypoxia-ischemia declines during brain maturation. *J Cereb Blood Flow Metab* 2000;20:1294–1300. [PubMed: 10994850]
11. Han BH, D'Costa A, Back SA, Parsadanian M, Patel S, Shah AR, Gidday JM, Srinivasan A, Deshmukh M, Holtzman DM. BDNF blocks caspase-3 activation in neonatal hypoxia-ischemia. *Neurobiol Dis* 2000;7:38–53. [PubMed: 10671321]
12. Nakajima W, Ishida A, Lange MS, Gabrielson KL, Wilson MA, Martin LJ, Blue ME, Johnston MV. Apoptosis has a prolonged role in the neurodegeneration after hypoxic ischemia in the newborn rat. *J Neurosci* 2000;20:7994–8004. [PubMed: 11050120]
13. Ankarcrona M, Dypbukt JM, Bonfoco E, Zhivotovsky B, Orrenius S, Lipton SA, Nicotera P. Glutamate-induced neuronal death: a succession of necrosis or apoptosis depending on mitochondrial function. *Neuron* 1995;15:961–973. [PubMed: 7576644]
14. Leist M, Single B, Castoldi AF, Kuhnle S, Nicotera P. Intracellular adenosine triphosphate (ATP) concentration: a switch in the decision between apoptosis and necrosis. *J Exp Med* 1997;185:1481–1486. [PubMed: 9126928]
15. Ferrer I, Pozas E, Lopez E, Ballabriga J. Bcl-2, Bax, and Bcl-x expression following hypoxia-ischemia in the infant rat brain. *Acta Neuropathol (Berl)* 1997;94:583–589. [PubMed: 9444360]
16. Cheng Y, Gidday JM, Yan Q, Shah AR, Holtzman DM. Marked age-dependent neuroprotection by brain-derived neurotrophic factor against neonatal hypoxic-ischemic brain injury. *Ann Neurol* 1997;41:521–529. [PubMed: 9124810]
17. Benjelloun N, Renolleau S, Represa A, Ben-Ari Y, Charriaut-Marlangue C. Inflammatory responses in the cerebral cortex after ischemia in the P7 neonatal rat. *Stroke* 1999;30:1916–1923. [PubMed: 10471445]comment 1923–1924
18. Derugin N, Ferriero DM, Vexler ZS. Neonatal reversible focal cerebral ischemia: a new model. *Neurosci Res* 1998;32:349–353. [PubMed: 9950062]

19. Derugin N, Wendland M, Muramatsu K, Roberts T, Gregory G, Ferriero D, Vexler Z. Evolution of brain injury after transient middle cerebral artery occlusion in neonatal rat. *Stroke* 2000;31:1752–1761. [PubMed: 10884483]
20. Paxinos, G.; Watson, C. *The Rat Brain in Stereotaxic Coordinates*. New York, NY: Academic Press; 1986.
21. Srinivasan A, Roth KA, Sayers RO, Shindler KS, Wong AM, Fritz LC, Tomaselli KJ. In situ immunodetection of activated caspase-3 in apoptotic neurons in the developing nervous system. *Cell Death Differ* 1998;5:1004–1016. [PubMed: 9894607]
22. Van Lookeren Campagne M, Verheul HB, Vermeulen JP, Balazs R, Boer GJ, Nicolay K. Developmental changes in NMDA-induced cell swelling and its transition to necrosis measured with 1H magnetic resonance imaging, impedance and histology. *Brain Res Dev Brain Res* 1996;93:109–119.
23. Dijkhuizen RM, van Lookeren Campagne M, Niendorf T, Dreher W, van der Toorn A, Hoehn-Berlage M, Verheul HB, Tulleken CA, Leibfritz D, Hossmann KA, Nicolay K. Status of the neonatal rat brain after NMDA-induced excitotoxic injury as measured by MRI, MRS and metabolic imaging. *NMR Biomed* 1996;9:84–92. [PubMed: 8887373]
24. van der Toorn A, Sykova E, Dijkhuizen RM, Vorisek I, Vargova L, Skobisova E, van Lookeren Campagne M, Reese T, Nicolay K. Dynamic changes in water ADC, energy metabolism, extracellular space volume, and tortuosity in neonatal rat brain during global ischemia. *Magn Reson Med* 1996;36:52–60. [PubMed: 8795020]
25. Moseley ME, Cohen Y, Mintorovitch J, Chileuitt L, Shimizu H, Kucharczyk J, Wendland MF, Weinstein PR. Early detection of regional cerebral ischemia in cats: comparison of diffusion- and T2-weighted MRI and spectroscopy. *Magn Reson Med* 1990;14:330–346. [PubMed: 2345513]
26. Roberts TP, Vexler Z, Derugin N, Moseley ME, Kucharczyk J. High-speed MR imaging of ischemic brain injury following stenosis of the middle cerebral artery. *J Cereb Blood Flow Metab* 1993;13:940–946. [PubMed: 7691853]
27. van Bruggen N, Cullen BM, King MD, Doran M, Williams SR, Gadian DG, Cremer JE. T2- and diffusion-weighted magnetic resonance imaging of a focal ischemic lesion in rat brain. *Stroke* 1992;23:576–582. [PubMed: 1373254]
28. Vexler ZS, Ayus JC, Roberts TP, Fraser CL, Kucharczyk J, Arief AI. Hypoxic and ischemic hypoxia exacerbate brain injury associated with metabolic encephalopathy in laboratory animals. *J Clin Invest* 1994;93:256–264. [PubMed: 8282795]
29. Felderhoff-Mueser U, Taylor DL, Greenwood K, Kozma M, Stibenz D, Joashi UC, Edwards AD, Mehmet H. Fas/CD95/APO-1 can function as a death receptor for neuronal cells in vitro and in vivo and is upregulated following cerebral hypoxic-ischemic injury to the developing rat brain. *Brain Pathol* 2000;10:17–29. [PubMed: 10668892]
30. Northington FJ, Ferriero DM, Flock DL, Martin LJ. Delayed neurodegeneration in neonatal rat thalamus after hypoxia-ischemia is apoptosis. *J Neurosci* 2001;21:1931–1938. [PubMed: 11245678]
31. Lankiewicz S, Marc Luetjens C, Truc Bui N, Krohn AJ, Poppe M, Cole GM, Saido TC, Prehn JH. Activation of calpain I converts excitotoxic neuron death into a caspase-independent cell death. *J Biol Chem* 2000;275:17064–17071. [PubMed: 10828077]
32. Dirnagl U, Iadecola C, Moskowitz MA. Pathobiology of ischaemic stroke: an integrated view. *Trends Neurosci* 1999;22:391–397. [PubMed: 10441299]
33. Lee JM, Grabb MC, Zipfel GJ, Choi DW. Brain tissue responses to ischemia. *J Clin Invest* 2000;106:723–731. [PubMed: 10995780]
34. Ferrer I, Tortosa A, Condom E, Blanco R, Macaya A, Planas A. Increased expression of bcl-2 immunoreactivity in the developing cerebral cortex of the rat. *Neurosci Lett* 1994;179:13–26. [PubMed: 7845608]
35. Renolleau S, Aggoun-Zouaoui D, Ben-Ari Y, Charriaut-Marlangue C. A model of transient unilateral focal ischemia with reperfusion in the P7 neonatal rat: morphological changes indicative of apoptosis. *Stroke* 1998;29:1454–1460. [PubMed: 9660403]comment 1461
36. Blomgren K, Zhu C, Wang X, Karlsson JO, Leverin AL, Bahr BA, Mallard C, Hagberg H. Synergistic activation of caspase-3 by m-calpain after neonatal hypoxia-ischemia: a mechanism of “pathological apoptosis”? *J Biol Chem* 2001;276:10191–10198. [PubMed: 11124942]

37. Barone FC, Hillegass LM, Price WJ, White RF, Lee EV, Feuerstein GZ, Sarau HM, Clark RK, Griswold DE. Polymorphonuclear leukocyte infiltration into cerebral focal ischemic tissue: myeloperoxidase activity assay and histologic verification. *J Neurosci Res* 1991;29:336–345. [PubMed: 1656059]
38. Wendland, M.; Derugin, N.; Manabat, C.; Vexler, ZS. Permeability of the blood-brain barrier differs in immature versus mature rats following transient focal cerebral ischemia; *Proceedings, Society for Neuroscience*; 2001.

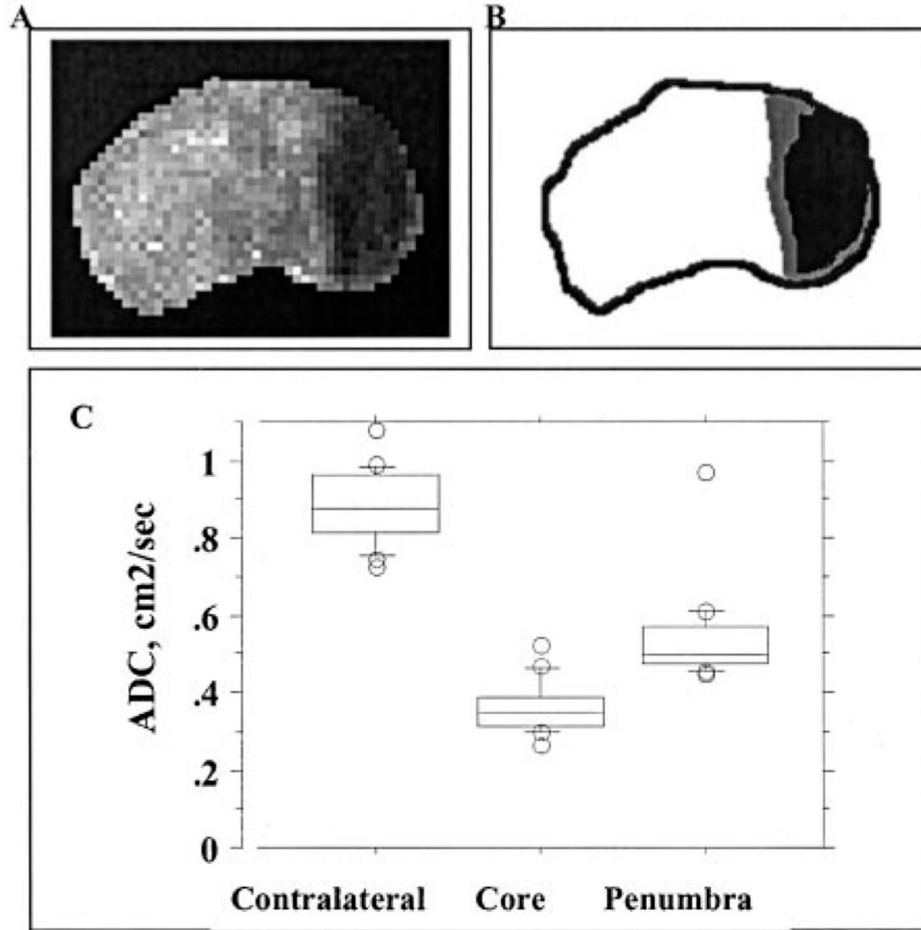


Figure 1. Acute changes in water diffusion after MCA occlusion in P7 rats. DW MRI was performed during suture MCA occlusion, and ADC maps were constructed. A, ADC map shows a well-outlined region of hypointensity in the injured brain regions. Note the gradual decrease in signal intensity at the edge of the core. B, Sketch of the ADC map shown in A. The ischemic core is demarcated in black, while penumbra is demarcated in gray. C, ADC values in the core, penumbra, and tissue in matching contralateral regions.

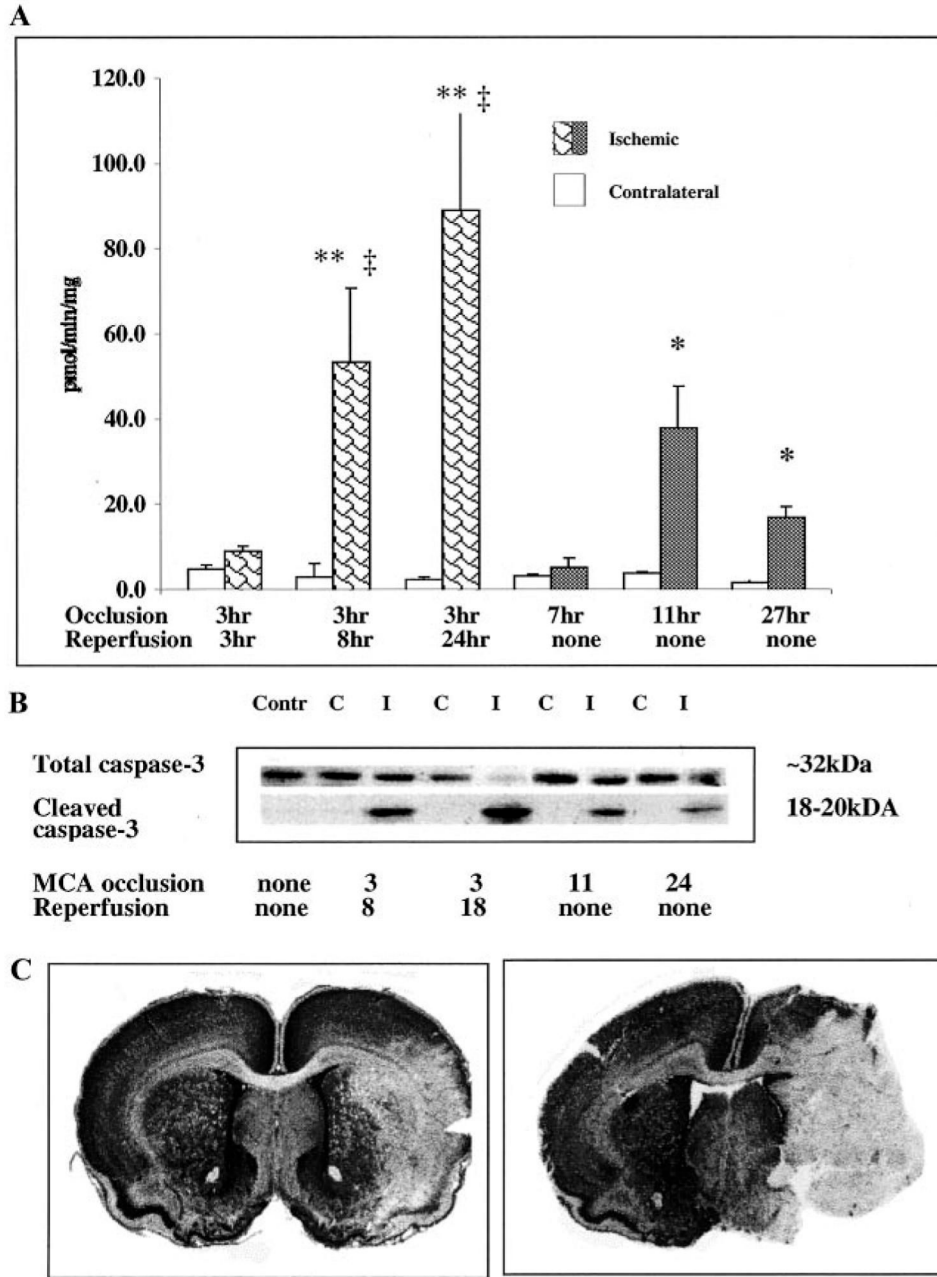


Figure 2. Caspase-3 activation occurs in injured tissue after focal cerebral ischemia in P7 rats and depends on the presence of reperfusion. DEVD-AMC assay (A) and Western blot analysis (B) were performed in brain homogenates obtained from the injured tissue and from tissue in matching contralateral regions. Tissue from the same brains was used for both assays. A, Caspase-3 activity was measured in DEVD-AMC cleavage assay with the use of Ac-DEVD as a substrate. Ac-AMC was used to obtain a standard curve. Enzyme activity is expressed as picomoles per minute per milligram protein. * $P < 0.01$, values in injured tissue vs values in matching regions of contralateral hemisphere; ** $P < 0.0001$, values in injured tissue vs values in matching regions of contralateral hemisphere; ‡ $P < 0.0001$, values in injured tissue after permanent MCA occlusion vs values in same hemisphere after the same duration of transient

MCA occlusion. B, Protein expression of pro-caspase-3 (top) and cleaved caspase-3 (bottom) was determined by Western blot analysis with the use of specific antibodies. Contr indicates control; C, contralateral; I, ipsilateral. C, Severity of injury 24 hours after transient (left) and 27 hours after permanent (right) MCA occlusion was determined by cresyl violet staining. Note that more severe injury after permanent MCA occlusion is accompanied by less caspase-3 activity (A) and caspase-3 cleavage (B).

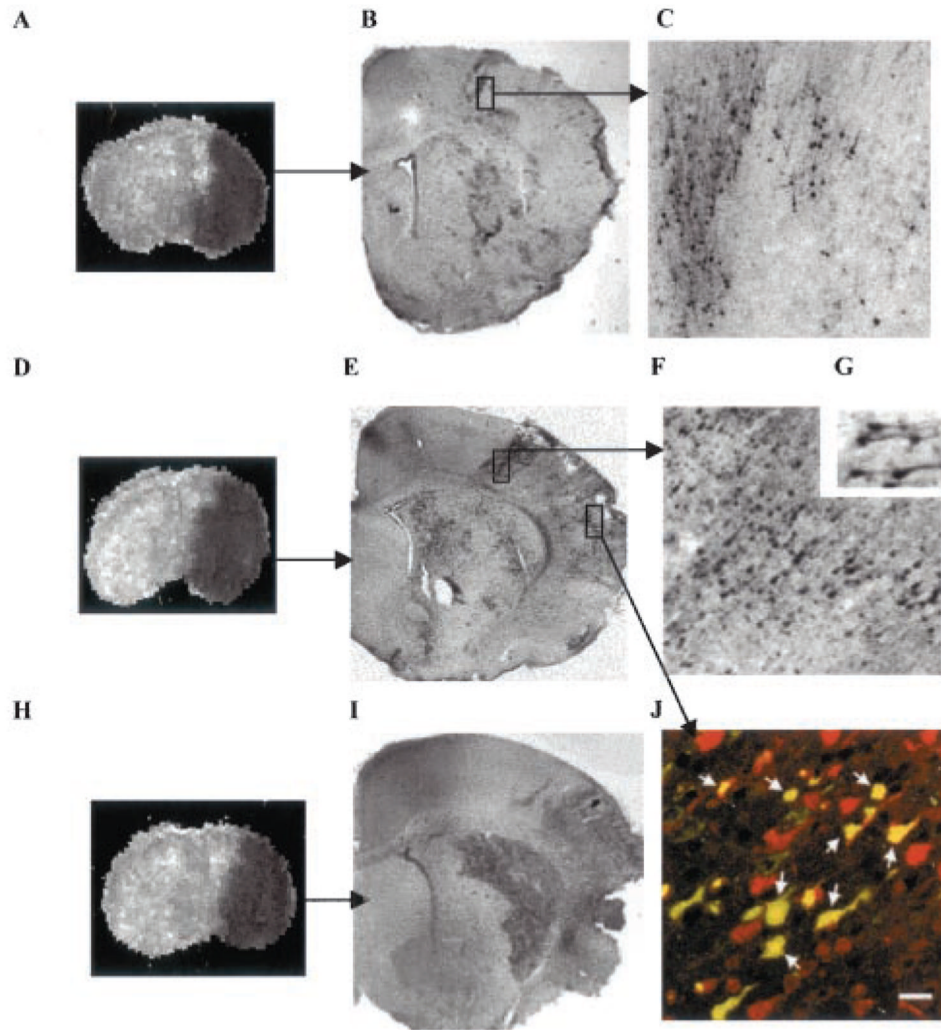


Figure 3.

Temporospatial distribution of cells with cleaved caspase-3 after transient MCA occlusion. A to C, ADC map (A) and CM1-immunoreactive cells (B and C) after 4 hours of reperfusion; D to G and J, ADC map (D) and CM1-immunoreactive cells (E to G, J) 8 hours after reperfusion. C and F are higher-magnification images from boxes shown in B and E. Insert G shows that both cell bodies and processes are intensely stained with CM1 antibody. H and I, ADC map (H) and CM1-immunoreactive cells (I) 24 hours after reperfusion. J, Immunofluorescent double labeling with a neuronal marker, NeuN (red) and CM1 (green). Confocal image from the cortex ipsilateral to MCA occlusion shows that caspase-3 activation occurs predominantly in neurons in injured brain tissue 8 hours after MCA occlusion. Arrows in J point to yellow cells in which CM1 and NeuN staining is colocalized. Bar=20 μ m.

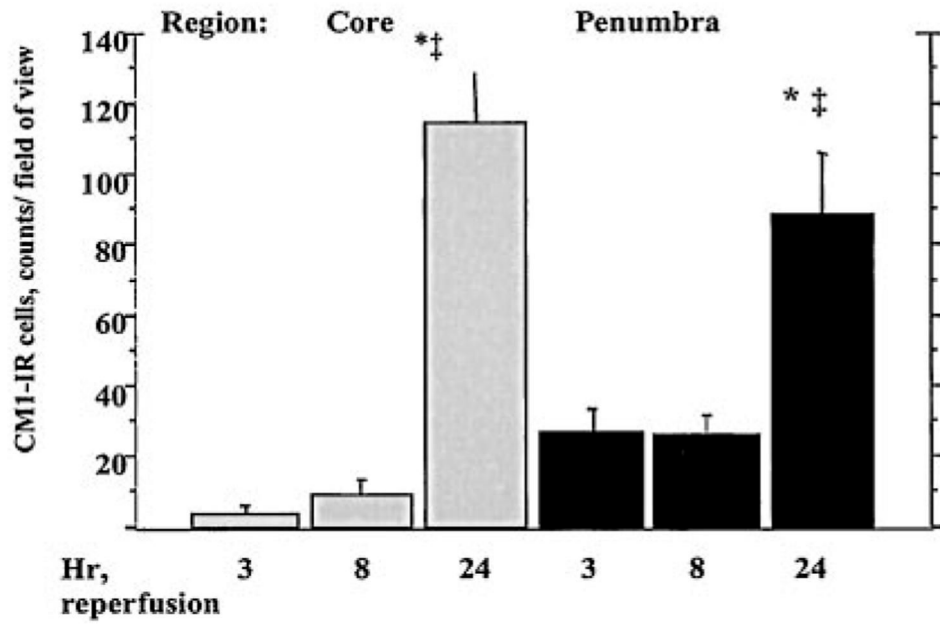


Figure 4. Activation of caspase-3 in immature brain after focal cerebral ischemia differs in the ischemic core and penumbra. Quantitative analysis of CM1-immunoreactive (CM1-IR) cells in the core and penumbra after transient MCA occlusion in P7 rat is shown. * $P < 0.05$, values in injured tissue vs values in matching regions of contralateral hemisphere; ‡ $P < 0.05$, values in injured tissue vs values in injured tissue 3 hours after reperfusion.